



# Reductive dechlorination of trichloroethylene by combining autotrophic hydrogen-bacteria and zero-valent iron particles

Shang-Ming Wang\*, Szu-kung Tseng

Graduate Institute of Environmental Engineering, National Taiwan University, No. 71 Chou-Shan Road, Taipei 106, Taiwan, ROC

## ARTICLE INFO

### Article history:

Received 19 February 2008

Received in revised form 22 May 2008

Accepted 23 May 2008

Available online 7 July 2008

### Keywords:

TCE

Zero-valent iron

Dechlorination

Autotrophic hydrogen-bacteria

## ABSTRACT

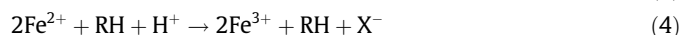
The objective of this study was to evaluate the dechlorination rate (from an initial concentration of  $180 \mu\text{mol l}^{-1}$ ) and synergistic effect of combining commercial  $\text{Fe}^0$  and autotrophic hydrogen-bacteria in the presence of hydrogen, during TCE degradation process. In the batch test, the treatment using  $\text{Fe}^0$  in the presence of hydrogen ( $\text{Fe}^0/\text{H}_2$ ), showed more effective dechlorination and less iron consumption than  $\text{Fe}^0$  utilized only ( $\text{Fe}^0/\text{N}_2$ ), meaning that catalytic degradation had promoted transformation of TCE, and the iron was protected by cathodic hydrogen. The combined use of  $\text{Fe}^0$  and autotrophic hydrogen-bacteria was found to be more effective than did the individual exercise even though the hydrogen was insufficient during the batch test. By the analysis of XRPD, the crystal of  $\text{FeS}$  transformed by sulfate reducing bacteria (SRB) was detected on the surface of iron after the combined treatment. The synergistic impact was caused by  $\text{FeS}$  precipitates, which enhanced TCE degradation through catalytic dechlorination. Additionally, the dechlorination rate coefficient of the combined method in MFSB was 3.2-fold higher than that of iron particles individual use. Results from batch and MFSB experiments revealed that, the proposed combined method has the potential to become a cost-effective remediation technology for chlorinated-solvent contaminated site.

© 2008 Elsevier Ltd. All rights reserved.

## 1. Introduction

Halogenated compounds, such as trichloroethylene (TCE) and perchloroethylene (PCE), are ubiquitous priority groundwater pollutants that pose a risk to public health. Most of these solvents are highly toxic; therefore, the remediation of polluted sites is desirable. The recalcitrance of halogenated compounds depends on number, position and type of the halogen substituents. Owing to the electro-negativity of the halogen atom, these organo-halogens are difficult to degrade via oxidative processes (Magnuson et al., 1998). Many of the halogenated solvents exist in the subsurface as dense non-aqueous phase liquids (DNAPLs) because of their densities and low water solubility; these physico-chemical characteristics make them difficult to remove, via the pump-and-treat method. Permeable reactive barriers (PRBs) containing zero-valent iron ( $\text{Fe}^0$ ) are becoming increasingly popular for in situ remediation of groundwater contaminated with chlorinated solvents (Matheson and Tratnyek, 1994; Burris et al., 1995; Orth and Gillham, 1996; Roberts et al., 1996; Wüst et al., 1999; Choe et al., 2001; Cervini et al., 2002). There are three major reaction pathways involved in the dechlorination of  $\text{Fe}^0$  (Matheson and Tratnyek, 1994; Burris et al., 1995; Orth and Gillham, 1996): (A)

direct electron transfer from iron surface (Eq. (1)); (B) catalyzed hydrogenolysis by hydrogen ( $\text{H}_2$ ), which is produced by reduction of  $\text{H}_2\text{O}$  during anaerobic iron corrosion (Eq. (5)); (C) reduction by  $\text{Fe}^{2+}$ , which is from corrosion of  $\text{Fe}^0$  (Eq. (4))



A potential limitation of the  $\text{Fe}^0$  remediation technology is the deterioration of the iron materials by corrosion and the subsequent precipitation of minerals, which may cause cementation and decreased the permeability of PRBs (Reardon, 1995; Gu et al., 1999; Heuer and Stubbins, 1999; Phillips et al., 2000; Agrawal et al., 2002; Ritter et al., 2002).

Since most of the contaminated sites are anaerobic, stimulation of reductive dehalogenation is a very promising strategy for bioremediation aquifers contaminated with halogenated compounds. Reductive dechlorination is either a cometabolic or a respiratory process (halorespiration), which is carried out by organochlorine-reducing bacteria. The dechlorination rates of the cometabolic processes are much lower than halorespiration (Yager et al., 1997), and their contributions to dehalogenation observed in natural

\* Corresponding author. Tel.: +886 918382492; fax: +886 2 23632637.

E-mail address: f89541101@ntu.edu.tw (S.-M. Wang).

environments are negligible. In contrast, organochlorine-reducing bacteria, which utilize chlorinated hydrocarbons as electron acceptors in energy metabolism and hence for growth are likely to be major contributors in anaerobic environments. Unfortunately, many laboratory and in situ observations show that most halo-respiring microorganisms produce *cis*-dichloroethene (*cis*-DCE) and vinyl chloride (VC) as terminal products. Only a few microorganisms can completely dechlorinate PCE and TCE to ethene or ethane (Maymó-gatell et al., 1995; Magnuson et al., 1998; Holliger et al., 1999). The fate of VC in field sites is of particular concern because the chlorinated ethene is a human carcinogen.

In recent years, several articles have been devoted to the study of combining  $\text{Fe}^0$  and cells to degrade chlorinated hydrocarbons (Weathers et al., 1997; Lee et al., 2001). These studies propose that the cathodic hydrogen produced from  $\text{Fe}^0$  can support dechlorination by microorganism. In other words, the  $\text{Fe}^0$  is merely used as a time-released hydrogen source and the cathodic hydrogen is utilized as an electron donor for respiratory dechlorination. Although the results reveal that the combined use of  $\text{Fe}^0$  and cells showed more effective dechlorination than did the individual use, the  $\text{Fe}^0$  still corroded after reaction. The sustainability of  $\text{Fe}^0$  remains a potential limitation for in situ remediation and mineral clogging would occur. This research is intended as an investigation of TCE dechlorination using  $\text{Fe}^0$  and autotrophic hydrogen-bacteria under hydrogen supplied environment. In this combined system, autotrophic hydrogen-bacteria utilized hydrogen to carry out halo-respiration, and  $\text{Fe}^0$  will be protected due to the high affinity with hydrogen (there will be a hydrogen coating around  $\text{Fe}^0$  particles). When the TCE is adsorbed on the surface of the  $\text{Fe}^0$ , catalytic dechlorination will occur, completely and rapidly, in the system (Eq. (5)), therefore, dechlorination could be achieved in this combined system. The objectives of this paper were; (1) to determine if zero-valent iron could accelerate TCE dechlorination via catalyzed hydrogenolysis; (2) to identify the reduction of iron consumption during this combined system; (3) to evaluate the dechlorination efficiency of TCE in a bioreactor with continuous hydrogen input. A serum bottle batch test was utilized to evaluate the dechlorination efficiency and corrosion of  $\text{Fe}^0$ ; a membrane feeding substrate bioreactor (MFSB) was set up to examine the removal of TCE with continuously supplied hydrogen.

## 2. Methods

### 2.1. Sludge, medium and growth conditions

The digest sludge, utilized in this research, was gathered from a livestock breeding wastewater treatment plant (mixed culture) and was incubated in the growth medium containing the following; (final concentration in grams per liter):  $\text{NaHCO}_3$ , 2.0;  $\text{KH}_2\text{PO}_4$ , 2.0;  $\text{MgSO}_4 \cdot 7\text{H}_2\text{O}$ , 0.148; *N*-(2-hydroxyethyl)-*N*-2-ethanesulfonic acid (HEPES), 11.2, and 1 ml of a trace metal solution comprising (grams per liter)  $\text{CaCl}_2 \cdot 2\text{H}_2\text{O}$ , 7.0;  $\text{MnCl}_2 \cdot 4\text{H}_2\text{O}$ , 2.5;  $\text{FeCl}_3$ , 1.8;  $\text{CoCl}_2 \cdot 6\text{H}_2\text{O}$ , 0.5;  $(\text{NH}_4)_2\text{Mo}_7\text{O}_{24} \cdot 2\text{H}_2\text{O}$ , 0.5;  $\text{CuCl}_2$ , 0.1. Before incubation, the growth medium was purged with  $\text{N}_2$  to avoid the interference of dissolved oxygen. Digest sludge was incubated in a sealed, continuously stirred reactor, which had a working volume of 2.4 l at 25 °C, purged with hydrogen, via a cylinder (10 ml/min). Pure TCE was injected into the incubation reactor, the initial TCE concentration was  $180 \mu\text{mol l}^{-1}$ . The pH of medium solution was adjusted by 20%  $\text{H}_3\text{PO}_4$  to approximately 7.0. The digest sludge was maintained by weekly transfer into a 250 ml serum bottle, which contained the same growth medium as the reactor, and the subculture had undergone 3 serial transfers before use.

### 2.2. Batch experiments

Commercial granular iron (purity > 99.5%, 100 mesh, Hognas) was chosen in this experiment. Because there is an oxidation layer on iron particles, before reactions, we immersed the iron into 1 M HCl solution for 24 h to remove impurities of the iron surface (Arnold and Roberts, 2000). Initially, the reactants ( $\text{Fe}^0$  or sludge) were put into 125 ml serum bottles and then filled with medium solution. Following this, the vials were subsequently sealed with Teflon-lined, butyl-rubber septa, and aluminum crimp caps. Then, the serum bottles were flushed with hydrogen or nitrogen gas through the septa to displace the medium solution (60 ml). Finally, TCE was added to the vials from Teflon septa with a 2  $\mu\text{l}$  GC sampling syringe and sealed with wax. The initial TCE concentration of the vials was  $180 \mu\text{mol l}^{-1}$ . All the well-sealed vials were incubated on a circular action shaker at 250 rpm (25 °C). With the exception of the sludge, all the materials (medium, serum bottles, Teflon septa, and sampling syringe) were autoclaved at 120 °C for 20 min before the experiment. A description of the batch experiment is shown in Table 1.

### 2.3. Membrane feeding substrate bioreactor (MFSB)

The bioreactor was constructed of Pyrex with an effective volume of 2.4 l. A gas-permeable silicone tube (1.5 mm [i.d.] and 2.5 mm [o.d.] by 11.5 m long; Fuji System Co., Japan) was wound around the glass pillar in the bioreactor. Zero-valent iron particles and hydrogen-bacteria were added to the reactor, which was completely stirred by a propeller. Hydrogen injected into the silicone tube was supplied with gas cylinders via mass controllers. When hydrogen flowed through the silicone tube, it would diffuse the growth medium solution. The dissolved hydrogen provides the energy source to autotrophic hydrogen-bacteria as well as forming a protective layer around the iron surface. Catalytic hydrolysis would proceed when TCE adsorbs on the iron (Eq. (5)). A membrane feeding substrate bioreactor (MFSB) was utilized to determine dechlorination efficiency of different treatments, when continuous hydrogen was supplied. When the reactor was running, it was

**Table 1**

The constituents of batch experiments

	Components			
	Headspace (ml)	TCE ( $\mu\text{mol l}^{-1}$ )	Contents of immobilization	
			$\text{Fe}^0$ (g)	Sludge (ml)
Set 1 ( $\text{Fe}^0 + \text{H}_2$ )	60	180	1.5	0
Set 2 ( $\text{Fe}^0 + \text{N}_2$ )	60	180	1.5	0
Set 3 (sludge + $\text{H}_2$ )	60	180	0	10
Set 4 ( $\text{Fe}^0$ + sludge + $\text{H}_2$ )	60	180	1.5	10
Set 5 (control)	60	180	0	0

Final mass of TCE in each serum bottle (125 ml) is  $22.5 \mu\text{mol}$  and the volume of headspace is 60 ml.

**Table 2**

Description of MFSB treatments

	Components			
	Headspace (ml)	TCE ( $\mu\text{mol l}^{-1}$ )	Contents of immobilization	
			$\text{Fe}^0$ (g)	Sludge (ml)
Set A ( $\text{Fe}^0 + \text{H}_2$ )	5	180	20	0
Set B ( $\text{Fe}^0 + \text{N}_2$ )	5	180	20	0
Set C (sludge + $\text{H}_2$ )	5	180	0	100
Set D ( $\text{Fe}^0$ + sludge + $\text{H}_2$ )	5	180	20	100
Set E (control)	5	180	0	0

filled with a medium solution (headspace is 5 ml) and kept in a water bath to maintain the temperature at 25 °C. TCE was injected through Teflon septa on the head of the reactor, the TCE concentration was 180  $\mu\text{mol l}^{-1}$ . Properties of the reactors are summarized in Table 2.

#### 2.4. Analytical methods

TCE, *cis*-DCE, VC, ethane, ethene, acetylene and hydrogen were detected by gas chromatography (GC) using headspace analysis. A 500  $\mu\text{l}$  side-port, gas-tight GC sampling syringe (Hamilton) was used to withdraw the gas sample from the headspace of the vials and bioreactors and then injected into the GC. TCE and the reaction products during the experiment (*cis*-DCE, VC, ethane, ethene, acetylene and methane) were analyzed using a Hewlett–Packard 5890 gas chromatography equipped with a flame ionization detector (GC/FID) and a GS-GasPro capillary column (60 m  $\times$  0.32 mm i.d., 0.25 mm film thickness GS-GasPro capillary column; J&W Scientific, Folsom, CA). The temperature of injector and detector were 200 and 300 °C, respectively. The temperature program was as follows: 28 °C hold 3.5 min, 15 °C  $\text{min}^{-1}$  to 115 °C no hold, 7 °C  $\text{min}^{-1}$  to 180 °C, hold 2 min. The column flow rate was 2.5  $\text{ml min}^{-1}$  and the detention time of each compound was:  $\text{CH}_4$ , 1.23 min;  $\text{C}_2\text{H}_4$ , 1.93 min;  $\text{C}_2\text{H}_6$ , 2.33 min;  $\text{C}_2\text{H}_2$ , 2.78 min; *trans*-DCE, 12.83 min; *cis*-DCE, 14.73 min; TCE, 16.41 min. Hydrogen was analyzed on a Hewlett–Packard 5890 gas chromatography equipped with a thermal conductivity detector (GC/TCD) (Weathers et al., 1997; Lee et al., 2001) using a packed column (3.2 mm by 3.05 m stainless steel packed with 100/120 carbon sieve-S-II, Supelco, Inc.), and the operation temperature was 150 °C isothermally.

Total iron consumption was quantified by a modified 1,10-phenanthroline test, as described by Marchand and Silverstein (2002). A 1-ml sample of suspension was collected, and then 9 ml of 10% HCl was added to the gathered samples to dissolve the colloid and precipitates. After 30-min digestion at 150 °C, 20 ml  $\text{NH}_2\text{OH} \cdot \text{HCl}$  (50  $\text{g l}^{-1}$ ) was injected into the samples to reduce  $\text{Fe}^{3+}$  to  $\text{Fe}^{2+}$ . Finally, 10% (v/v) of a 2.0  $\text{g l}^{-1}$  solution of 1,10-phenanthroline was added to react with  $\text{Fe}^{2+}$ . The color was measured at 510 nm in a spectrophotometer (Thermo, Spectronic 20D) after a 15-min reaction time. The analysis of sulfate was measured using a Dionex 120 ion chromatography (IC) system with a Dionex Ionpac AS-16 column after filtration (0.22  $\mu\text{m}$  filter, Millipore). Samples, which reacted with microorganisms, required centrifuge before filtration and IC analysis.

Scanning electron microscopy energy dispersive X-ray (SEM-EDX) and X-ray powder diffraction (XRPD) were introduced to identify the chemical constituents and crystal phases of the precipitates, which was gathered from bioreactors and vials. Samples were stored under He atmosphere at  $-20$  °C until analysis of XRPD and EDX. After drying, samples were shaken onto amorphous carbon film and supported by a copper adapter to avoid electrical charging during analysis. The samples were observed using the bright-field imaging mode of SEM (Topcon ABT-150s) with an acceleration voltage of 15 kV, at a take-off angle of 47.76°. XRPD (Regaku D/max-II B) was performed with 35 kV and 20 mA current from 5° to 90° (2 $\theta$ ) at a scanning speed of 4°  $\text{min}^{-1}$  to identify the crystal phases of the precipitates.

### 3. Results and discussion

#### 3.1. Dechlorination of the batch test

The plot of TCE concentration against reaction time in the batch vials under different incubation conditions are shown in Fig. 1. Sets 1 and 2 were treated with identical concentrations of iron powder,

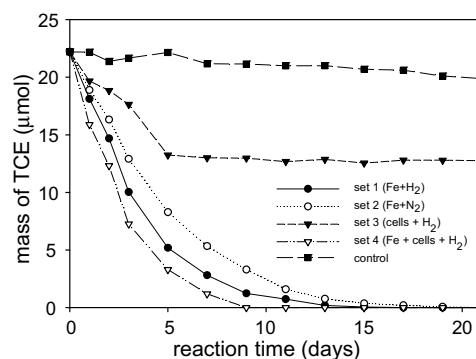


Fig. 1. The mass of TCE against reaction time in batch test under different incubation conditions. The initial TCE mass in serum bottle was 22.5  $\mu\text{mol}$  (180  $\mu\text{mol l}^{-1}$ ).

but supplemented with different source gases in the headspace of each set of vials. Hydrogen gas was added to set 1 rather than set 2 in order to investigate if TCE dechlorination would be enhanced by catalyzed hydrogenolysis in the presence of hydrogen. Initially, the TCE in both vials containing only  $\text{Fe}^0$  obtained high removal efficiency; however, after two days of incubation, the degradation rate in  $\text{Fe}^0/\text{N}_2$  vials decreased slightly, whereas TCE transformation in  $\text{Fe}^0/\text{H}_2$  vials continued to react rapidly. The efficiency of dechlorination varied in the later period based on different types of gas-filled headspace. The TCE degradation mechanism in set 2 was mainly concerned with iron corrosion (Eqs. (1)–(4)); while set 1 was correlated most strongly with catalytic dechlorination, because set 1 was prevented from the severe corrosion of iron with the hydrogen-filled headspace. In comparison, catalytic dechlorination would be the main reaction mechanism in set 1. It was observed that, greater than 99% of the added TCE were degraded in set 1 ( $\text{Fe}^0/\text{H}_2$ ) within 13 days, however, the same degradation was achieved in set 2 ( $\text{Fe}^0/\text{N}_2$ ) in 18 days. These results suggested that the treatment with  $\text{Fe}^0$  could be dechlorinated much more rapid in the presence of hydrogen.

Digested sludge and hydrogen gas were introduced into set 3 for examination of the effect of hydrogen–bacteria on TCE biodegradation, via halo-respiration. As shown in Fig. 1, the TCE degradation rate was significantly enhanced by the sludge incubated in set 3 after a lag period of two days. Unfortunately, the biodegradation of TCE ceased after seven days of reaction, because of a hydrogen shortage in the headspace (more details on hydrogen concentration will be provided in the later section). The cells showed that 42% of the added TCE (9.3  $\mu\text{mol}$ ) was degraded during 21 days of incubation; yet complete biodegradation was almost obtained after only 7 days of incubation, as illustrated in Fig. 1, indicating that the later reaction came close to a halt. Accordingly, it was assumed that the treatment with the cells might be degraded in a better manner with a sufficient supply of hydrogen.

Set 4 was added with  $\text{Fe}^0$ , digested sludge, and a hydrogen supplement to the headspace. The results as shown in Fig. 1 suggest that the combined use and concurrent treatment of  $\text{Fe}^0$  and autotrophic hydrogen–bacteria exhibited the fastest degradation rate to remove most of the TCE within 10 days. In addition, Fig. 1 also shows that the length of the reaction time would not reduce the efficiency of set 4, in contrast, TCE degradation in set 2 might become negligible, a result of iron corrosion in the post period. As for control vials containing medium solution with hydrogen-filled headspace (set 5), the emission concentrations of TCE revealed less than 5% total over the duration of the batch test. Abiotic loss and degradation of indigenous population in medium solution or vials might be the major reason for TCE decrease, which is too slight to be significant.

When TCE concentrations, as shown in Fig. 1, were plotted as  $\ln(C_t/C_0)$  versus  $t$  (where  $C_t$  is TCE concentration at reaction time  $t$ , and  $C_0$  refers to the initial concentration of TCE), the data produced linear plots, indicating that TCE degradation followed first order kinetics (non-linear data in lag-phase and steady-state data are not included). The slopes of these plots were equivalent to the pseudo-first-order rate coefficient in each set. The TCE degradation rate coefficient for the treatment of each set is as follows:  $0.36 \text{ day}^{-1}$  ( $r^2 = 0.97$ ) for  $\text{Fe}^0$  and hydrogen (set 1),  $0.24 \text{ day}^{-1}$  ( $r^2 = 0.98$ ) for  $\text{Fe}^0$  and nitrogen (set 2),  $0.08 \text{ day}^{-1}$  ( $r^2 = 0.95$ ) for cells only (set 3), and  $0.48 \text{ day}^{-1}$  ( $r^2 = 0.99$ ) for combined use of  $\text{Fe}^0$  and cells in presence of hydrogen (set 4).

The dechlorination intermediates, products types, and TCE concentrations against reaction time in each set are shown in Figs. 2–4. From Fig. 2, it is revealed that, *cis*-DCE was the most com-

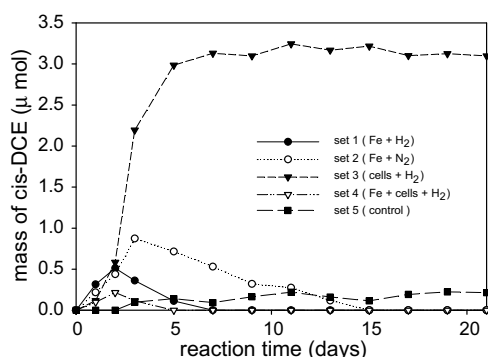


Fig. 2. The mass of *cis*-DCE against reaction time in batch test under different incubation conditions.

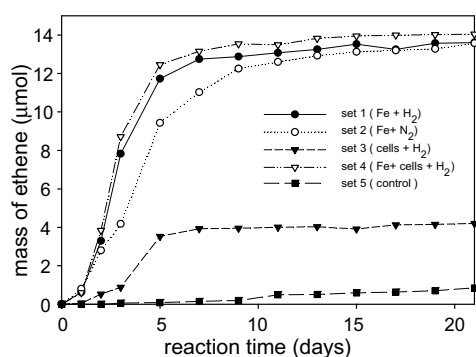


Fig. 3. The mass of ethene against reaction time in batch test under different incubation conditions.

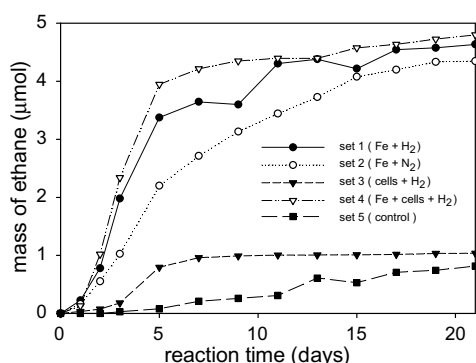


Fig. 4. The mass of ethane against reaction time in batch test under different incubation conditions.

mon intermediate in all dechlorination treatments during the experiment. In set 2, the accumulation of *cis*-DCE rose to a peak of  $1 \mu\text{mol}$  on the 3rd day, and then gradually degraded to ethane, or ethene, until the concentration of *cis*-DCE fell below the detection limit on 15th day, indicating that *cis*-DCE was a reactive intermediate during  $\text{Fe}^0$  treatment, and hence could be completely dechlorinated. Although similar trends were observed in set 1, it revealed far less accumulated *cis*-DCE (about  $0.5 \mu\text{mol}$ ), and a more rapid disappearance of *cis*-DCE in the catalytic dechlorination system; thus, no additional *cis*-DCE accumulation could be found on 7th day in set 1. That is to say, the transformation of *cis*-DCE would be accelerated by catalyzed hydrogenolysis, as compared with traditional  $\text{Fe}^0$  treatments, as in set 2). Formation and accumulation of *cis*-DCE were observed in the biological vials of set 3, which exhibited a dramatic increase in the concentration of *cis*-DCE, rising to the maximum on the 9th day (over  $3 \mu\text{mol}$ ), and being persistent in vials to the end of incubation. The results showed that autotrophic hydrogen-bacteria reacted worse to the dechlorination intermediates, with the possibility of being influenced by biological toxicity, referring to the difficulty of complete dechlorination proceedings, via simple cells. Rapid formation and disappearance of *cis*-DCE was observed in the vials containing  $\text{Fe}^0$  and cells with hydrogen (Fig. 2), with highest concentration ( $0.24 \mu\text{mol}$ ) after two days and complete disappearance after five days. In comparison with  $\text{Fe}^0$ -only in a biological system, these evidences support the hypothesis of the higher reactivity of the combined system on dechlorination, and transformation, of chlorinated metabolites.

In each set of batch experiments, ethane and ethene accumulation were shown as end products of TCE transformation, in addition, a low-concentration of methane was produced. The concentration-versus-time profiles of ethane and ethene in batch experiments are displayed in Figs. 3 and 4. Treatments with  $\text{Fe}^0$  and hydrogen-bacteria revealed the highest extent in accumulation of ethane and ethene among the five sets of vials. This represents that the most complete dechlorination occurred within the combined system, namely, the disappeared TCE in these vials was totally converted to non-chlorinated hydrocarbons (ethane and ethene). However, the composition of the products in biological treatment (set 3) was largely different from the combined system. In set 3, merely 55% of the disappeared TCE was converted into non-chlorinated hydrocarbons (ethane and ethene), and nearly 33% of that transformed to *cis*-TCE; undeniably, it could be the lack of hydrogen in the vials that counts for the lower reductive capability of biodechlorination.

The results from Fig. 1 revealed that, 42% TCE was removed in Set 3, however, the TCE removal mechanisms involved halorespiration and cell-adsorption, meaning that only a part of removed TCE was reduced through biodegradation. From the above, the TCE was decomposed to *cis*-DCE, ethane and ethene; therefore, the amount of TCE adsorbed on sludge could be estimated by mass balance of residual TCE and dechlorination products. According to Figs. 2–4, the mass of *cis*-DCE, ethane, and ethene were  $3.0$ ,  $3.9$ , and  $0.9 \mu\text{mol}$ , respectively. The total amount of carbon contained in these products was  $15.6 \mu\text{mol}$  (each mole product contains two moles of carbon). The amount of TCE degraded in set 3 was  $9.3 \mu\text{mol}$  ( $18.6 \mu\text{mol}$  of carbon), meaning that the difference between mass balance and degradation was  $1.5 \mu\text{mol}$  of TCE ( $3.0 \mu\text{mol}$  of carbon). Hence, the TCE adsorbed by sludge was approximately  $1.5 \mu\text{mol}$  (6.7%). In other words, only 35.3% TCE ( $7.8 \mu\text{mol}$ ) was actually degraded by cells.

### 3.2. Impacts of hydrogen concentration on batch tests

Hydrogen is an excellent energy source in a variety of autotrophic anaerobes, such as methanogens, sulfate reducers and halorespirers (Holliger et al., 1999; Gu et al., 1999). Therefore, suf-



ficient supply of hydrogen would be a primary factor for halofermentation. In this study, in addition to being regarded as an electron donor during biological dechlorination, hydrogen also played the important roles of reducer, in the catalytic dechlorination (Eq. (5)), as well as reducing gas in protection of iron oxidation. From the results of hydrogen concentration analysis, as detected by GC-TCD, show that 30% of the added hydrogen was preserved in vials of set 1 to the end of the treatment, meaning that the hydrogen supply in the headspace was abundant for catalytic hydrogenolysis (not shown in figures). The treatment containing cells only (set 3) had exhausted the supply of hydrogen in vials within 8 days, and consequently, the biological dechlorination ceased along with a great accumulation of *cis*-DCE (Fig. 2). From Figs. 3 and 4, it was obvious that the autotrophic hydrogen-bacteria introduced in this experiment could degrade TCE to non-chlorinated metabolite (ethane and ethene), hence the lower efficiency of TCE degradation and the accumulation of *cis*-DCE during the latter stage of reaction in set 3, were strongly dependent on the lack of hydrogen. The hydrogen consumption in the combined use of  $\text{Fe}^0$  and microorganisms (set 4) would be higher than set 1 or 3 because of hydrogen supply in biodegradation and catalytic hydrogenolysis. From the results of hydrogen analysis, we found that hydrogen was almost exhausted within 7 days in set 4; nevertheless, extremely low levels of hydrogen (3.4–4.5  $\mu\text{mol}$ ) in the headspace of vials was detected during the 7th–21st day of treatment. The production of hydrogen via fermentation could be neglected because there were no other organic substances in this reaction system, except for TCE and its metabolites. Several previous studies have reported that  $\text{Fe}^0$  corrosion in water could support continuous release of cathodic hydrogen, which provide an energy source of microorganisms for halofermentation (Weathers et al., 1997; Lee et al., 2001). In our experiments,  $\text{Fe}^0$  began to corrode when the hydrogen protection layer disappeared (set 4 had almost exhausted hydrogen within 7 days), therefore, it seems reasonable to suppose that the produced hydrogen after 7 days in set 4 was released from  $\text{Fe}^0$  corrosion. Supposing the residual TCE in set 4 after 7 days was degraded by  $\text{Fe}^0$  corrosion and halofermentation (hydrogen is supplied by  $\text{Fe}^0$  corrosion), then accumulation of *cis*-DCE and a slower rate of degradation in the initial stage could be expected. From Figs. 1 and 2, however, the combined system showed rapid dechlorination with no *cis*-DCE accumulation after 7 days of incubation. This observation suggested that TCE was probably dechlorinated via another mechanism, in addition to  $\text{Fe}^0$  corrosion and halofermentation in the late reaction period. The specific reaction mechanism able to achieve rapid, and complete dechlorination, will be discussed in the following section.

### 3.3. The synergistic effect of combined use of autotrophic hydrogen-bacteria and $\text{Fe}^0$

Results of batch studies demonstrated that TCE could be dechlorinated and transformed to ethane and ethene in very low hydrogen concentrations during the late reaction period in this combined system (set 4). This may be attributed to different hydrogen concentrations and changes in the chemical properties of an iron surface; and any variations in hydrogen levels in the combined system should be the most noticeable contributing factors. In natural ecosystems, hydrogen is an important intermediate in the anaerobic degradation of organic matter. In addition, competition exists due to the limited supply of hydrogen produced by fermentation. The production of hydrogen in a microbial system is generally believed to be the rate-limiting step. In the initial stage of batch tests, hydrogen in headspace was sufficient for catalytic hydrogenolysis and TCE biodegradation, via halofermentation (set 4). However, after 7 days of incubation, heterogeneous catalytic dechlorination and halofermentation had utilized most of the hydro-

gen in the headspace, and then  $\text{Fe}^0$  began to corrode with the last- ing liberation of cathodic hydrogen. Therefore, the rate of hydrogen production became the rate-limiting step, and competition for the limited supply of hydrogen produced from iron corrosion existed in all types of hydrogen-consuming microorganisms in the combined system, such as iron reduction, sulfate reduction, chloroethylene reduction, and methanogenic. Vials, which degraded TCE to *cis*-DCE and non-chlorinated hydrocarbons (ethane and ethene) after treatment of autotrophic hydrogen-bacteria (set 3), were analyzed by ion chromatography. The results showed that 95% of the sulfate initially added was preserved in vials after 21-days treatment (data not shown in figures). As illustrated in set 3, the primary biological reaction was halofermentation rather than sulfate reduction. However, there was a significant difference in the sulfate degradation rate between set 3 and set 4. From Fig. 5, we can find that sulfate in set 4 on the 5th day began to decrease as soon as the hydrogen concentration was gradually made inadequate. Moreover, a sudden drop in sulfate concentration was observed after 7 days of reaction when the hydrogen level was below 5  $\mu\text{mol}$  (Fig. 5). The decrease of sulfate in set 4 showed that sulfate reduction had replaced dechlorination, and played a predominant role in the biological reaction during the later period of incubation. The distinction between sets 3 and 4, in the post period, existed in the low-level hydrogen produced from iron corrosion in set 4, a concentration that makes sulfate reducers reactive.

After reduction of sulfate, a large amount of sulfide was produced in the vials. The ferrous iron from iron corrosion precipitated with  $\text{S}^{2-}$ , and then  $\text{FeS}$  settled on the surface of the iron particles (Eqs. (6) and (7)). Precipitates of  $\text{FeS}$ , or other sulfides, may be deposited on the surface of iron particles.



Hassan (2000) has proposed that TCE would be dechlorinated at a faster rate by combined use of ferrous sulfide and  $\text{Fe}^0$ , rather than  $\text{Fe}^0$  individually utilized. It also illustrated that, metallic iron acted as a source of molecular hydrogen, through its reaction with water, while iron sulfide behaved as the reaction site (catalyst) in this system – i.e. molecular hydrogen is necessary for dechlorination to occur. Ethene and ethane were the major products via the treatment with  $\text{FeS}/\text{Fe}^0$  and results showed that,  $\text{FeS}$  that degraded TCE in the presence of hydrogen, exhibited approximately 20-fold higher reaction rate than  $\text{Fe}^0$  did. Furthermore, it also confirmed the relationship between sulfur content and its dehalogenation capacity. In the present study, SEM-EDX was utilized to analyze the sulfur content of the iron surface. The EDX spectrum of iron particles incubated in set 4 for 21 days indicated that the sulfur content reached to 28.4% (the initial sulfur content of the iron particles was less than

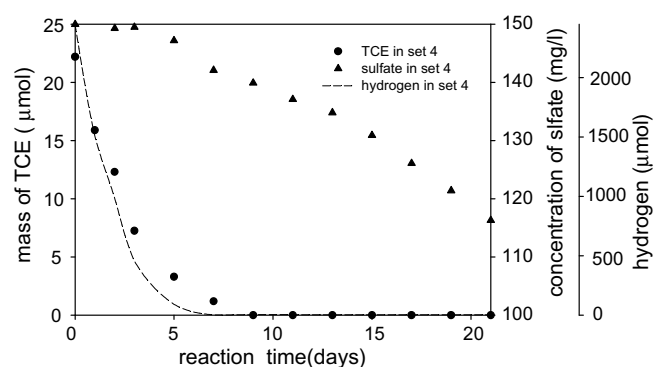


Fig. 5. The contents of TCE, hydrogen and sulfate concentration against reaction time in set 4 ( $\text{Fe} + \text{cells} + \text{H}_2$ ).

0.5%). Application of XRPD was adopted in this research to identify the crystal phase of iron particles. The iron particles were ground into powders in an agate mortar and then analyzed with XRPD. The XRPD pattern showed a clear peak at  $45.12^\circ$  ( $2\theta$ ), indicating the presence of FeS on the iron surface (data not shown in figures). All observations indicated that dechlorination, via FeS and cathodic hydrogen released by iron corrosion occurred in the combined system. For this reason, the dechlorination rate did not slow when hydrogen was nearly exhausted in the headspace. A low level of hydrogen produced by  $\text{Fe}^0$  corrosion was sufficient for catalytic hydrogenolysis to occur ( $\text{FeS}/\text{H}_2$ ).

#### 3.4. The consumption of $\text{Fe}^0$

The oxidative dissolution of iron particles occurred at neutral pH according to the characteristic reaction of iron corrosion (Eq. (3)). In the absence of oxygen, iron corrosion occurs, with water as an oxidant, under anaerobic conditions according to Eq. (3). As mentioned above, it is easy to know that a large amount of ferrous and hydroxyl ion are released with a conventional treatment of  $\text{Fe}^0$ . The degree of iron corrosion could be estimated by analyzing the accumulation of iron species ( $\text{Fe}^{2+}$ ,  $\text{Fe}^{3+}$ , colloid and precipitates) in a medium solution, after incubation. Fig. 6 shows profiles of iron consumption in vials with reaction time under different treatment. The incubation of set 2 ( $\text{Fe}^0/\text{N}_2$ ), which degraded TCE analogously to conventional  $\text{Fe}^0$  treatment, showed the most rapid corrosion rate of iron, as shown in Fig. 6. The iron consumption in set 2 initially increased sharply, then slowed during the late stages, probably owing to the precipitation of iron oxyhydroxides on the iron surface (Reardon, 1995; Gu et al., 1999); however, treatment of set 1 presented less oxidation of iron during reductive dechlorination of TCE. This proved that hydrogen did prevent iron from oxidizing, and that TCE was degraded mostly via catalyzed hydrolysis in set 1. In addition, it demonstrated again that the dechlorination mechanism between set 1 and set 2 were entirely different, as based on distinct corrosion levels. The  $\text{Fe}^0$  in set 2 oxidized almost 9-fold faster than in set 1. In contrast to set 1, similar trends of iron corrosion rates were observed in the combined system (set 4) during the first five reaction days, however, this was followed by a sudden increase in corrosion rate after seven days of incubation. According to the hydrogen profiles in Fig. 5, the corrosion rate of iron might be accelerated by inadequate hydrogen supply in the vials. Furthermore, the increase of iron consumption in the later period of set 4 suggested that, the possibility of the low level of hydrogen was produced by iron corrosion. As compared with set 2, the iron consumption of set 1 and set 4 were 11.5% and 53.1% of set 2, respectively.

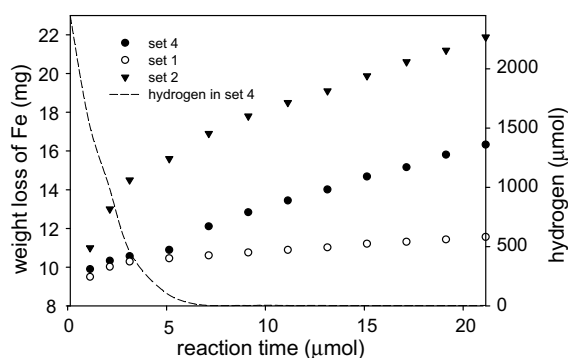


Fig. 6. The weight loss of Fe in set 1 ( $\text{Fe} + \text{H}_2$ ), set 3 (cells +  $\text{H}_2$ ) and set 4 ( $\text{Fe} + \text{cells} + \text{H}_2$ ) during dechlorination. The dotted line is the hydrogen contents of set 4 ( $\text{Fe} + \text{cells} + \text{H}_2$ ) against reaction time.

#### 3.5. Dechlorination of TCE in the MFSB

In the previous section, we pointed out that the supply of hydrogen was inadequate in the treatment of biological (set 3) and combined system (set 4). The membrane feeding substrate bioreactor (MFSB) was utilized to estimate the efficiency of dechlorination with continuous hydrogen production under different treatments. The experiment conditions remained the same as those of batch incubation, in addition to the manner in which hydrogen was supplied. The reactor containing  $\text{Fe}^0$  with continuous hydrogen production (set A) dechlorinated TCE completely within 30 days of treatment (data not shown in figures). The dechlorination rate constant for the reaction was  $0.15\text{-day}^{-1}$  ( $r^2 = 0.97$ ). Compared with set A, a similar reaction rate in set B was displayed in the earlier stage of incubation, however, it increased more slowly during the rest period of reaction, which may have been caused by passivation of  $\text{Fe}^0$  due to corrosion and precipitation of minerals. The rate constant for reaction of set B was  $0.09\text{-day}^{-1}$  ( $r^2 = 0.97$ ). For the duration of the treatment in set B, *cis*-DCE appeared in the first ten days, and then disappeared through the reduction of iron (the *cis*-DCE data was not displayed in figures). Roughly, 98% of the added TCE was transformed into ethane and ethene till the termination of the reaction.

The performance of biodegradation was greatly improved in MFSB with continuous supply of hydrogen. After a lag phase of three days, the biodegradation of TCE became much faster in set C. Only 4.8% of the added TCE was preserved in the bioreactor within 30 days of incubation, and the rate constant for the reaction of set C was  $0.08\text{-day}^{-1}$  ( $r^2 = 0.94$ ). The dechlorination efficiency of cells arose in MFSB, nevertheless, the accumulation of *cis*-DCE was still detected during the treatment (data not shown). At the end of the reaction, *cis*-DCE was accumulated to  $28.2\text{ }\mu\text{mol l}^{-1}$  in the bioreactor. The sludge-adsorption was estimated by the same manner described above, which showed that the amount of TCE adsorption was  $9.3\text{ }\mu\text{mol l}^{-1}$  (5.2%). The combined use of  $\text{Fe}^0$  and hydrogen autotrophic bacteria (set D) displayed the best capacity of TCE degradation (also obtained in set 4). Complete dechlorination was achieved in set D within 16 days of incubation. The rate of dechlorination in set D was up to  $0.29\text{ day}^{-1}$  ( $r^2 = 0.89$ ). However, the results of statistics revealed that the data of set D did not fully conform to pseudo-first-order kinetics ( $r^2 = 0.89$ ). The results of MFSB indicated that, the dechlorination of set D could be divided into two stages. The first stage, in which the rate of dechlorination was  $0.14\text{ day}^{-1}$  ( $r^2 = 0.98$ ), covered the period from the start of the reaction to the 5th day. The second stage was from the 5th day to the 13th day of set D, and the rate constant for the reaction was  $0.41\text{ day}^{-1}$  ( $r^2 = 0.98$ ). These observations could be illustrated with the results of the batch test. In the first stage, TCE was dechlorinated mostly by catalyzed hydrogenolysis and biological degradation. Compared with stage 1, in addition to the mechanisms mentioned above, the catalytic dechlorination by FeS, which was produced from the sulfate reduction, could exist in stage 2. It is noteworthy that, the concentration of sulfate in set D decreased by  $34.1\text{ mg l}^{-1}$  within 30 days of treatment (data not shown), and that the sulfur content on the iron surface, as detected by SEM-EDX, was 24.2%. In addition, FeS was found on the surface of iron particles from the qualitative analysis of XRPD (data not shown). These results confirmed that, the catalytic dechlorination proceeded via FeS and hydrogen should exist in the combined system and do accelerate the reaction rate in the later period of set D.

#### 4. Conclusion

Results showed that the combined use of  $\text{Fe}^0$  and autotrophic hydrogen-bacteria did have benefits of removing TCE. In summary,

the significant achievements obtained in this study were; (a) the dechlorination efficiency of  $\text{Fe}^0$  was improved in the presence of hydrogen; (b) the consumption of iron was reduced in virtue of the protection of hydrogen; (c) the combined use of  $\text{Fe}^0$  and cells enhanced the dechlorination of TCE by 320%, as compared with the conventional treatment of  $\text{Fe}^0$  in MFSB, and no chlorinated metabolite accumulated in this system; (d) the FeS produced from sulfate reduction had positive synergistic impacts on TCE degradation.

## Acknowledgements

This research was funded by the National Science Council of the Republic of China and the Contrast Number is NSC93-2211-E-002-031.

## References

- Agrawal, A., Ferguson, W.J., Gardner, B.O., Christ, J.A., Bandstra, J.Z., Tratnyek, P.G., 2002. Effect of carbonate species on the kinetics of dichloroethene by zero-valent iron. *Environ. Sci. Technol.* 36, 4326–4333.
- Arnold, W.A., Roberts, A.L., 2000. Pathways and kinetics of chlorinated ethylene and chlorinated acetylene reaction with  $\text{Fe}^0$  particles. *Environ. Sci. Technol.* 34, 1794–1805.
- Burris, D.R., Campell, T.J., Manoranjan, V.S., 1995. Sorption of trichloroethylene and tetrachloroethylene in a batch reactive metallic iron–water system. *Environ. Sci. Technol.* 29, 2850–2855.
- Cervini, J., Larson, R.A., Wu, J., Stucki, J.W., 2002. Dechlorination of pentachloroethane by commercial Fe and Ferruginous smectite. *Chemosphere* 47, 971–976.
- Choe, S., Lee, S., Chang, Y., Hwang, K., Khim, J., 2001. Rapid reductive destruction of hazardous organic compounds by nanoscale  $\text{Fe}^0$ . *Chemosphere* 42, 367–372.
- Gu, B., Phelps, T.J., Liang, L., Dickey, M.J., Roh, Y., Kinsall, B.L., Palumbo, A.V., Jacobs, G.K., 1999. Biological dynamics in zero-valent iron columns: implications for permeable reactive barriers. *Environ. Sci. Technol.* 33 (13), 2170–2177.
- Hassan, S.M., 2000. Reduction of halogenated hydrocarbons in aqueous media: involving of sulfur in iron catalysis. *Chemosphere* 40, 1357–1363.
- Heuer, J.K., Stubbins, J.F., 1999. An XPS characterization of  $\text{FeCO}_3$  films from  $\text{CO}_2$  corrosion. *Corros. Sci.* 41, 1231–1243.
- Holliger, C., Wohlfarth, G., Diekert, G., 1999. Reductive dechlorination in the energy metabolism of anaerobic bacteria. *FEMS Microbiol. Rev.* 22, 383–398.
- Lee, T., Tokunaga, T., Suyama, A., Furukawa, K., 2001. Efficient dechlorination of tetrachloroethene in soil slurry by combined use of an anaerobic *Desulfitobacterium* sp. Strain Y-51 and zero-valent iron. *J. Biosci. Bioeng.* 92 (5), 453–458.
- Magnuson, J.K., Stern, R.V., Gossett, J.M., Zinder, S.H., Burris, D.R., 1998. Reductive dechlorination of tetrachloroethene to ethene by a two-component enzyme pathway. *Appl. Environ. Microbiol.* 64 (4), 1270–1275.
- Marchand, E.A., Silverstein, J., 2002. Influence of heterotrophic microbial growth on biological oxidation of pyrite. *Environ. Sci. Technol.* 36, 5483–5490.
- Matheson, L.J., Tratnyek, P.G., 1994. Reductive dehalogenation of chlorinated methanes by iron metal. *Environ. Sci. Technol.* 28, 2045–2053.
- Maymó-gatell, X., Tandoi, V., Gossett, J.M., Zinder, S.H., 1995. Characterization of an  $\text{H}_2$ -utilizing enrichment culture that reductively dechlorinates tetrachloroethene to vinyl chloride and ethene in the absence of methanogenesis and acetogenesis. *Appl. Environ. Microbiol.* 61, 3928–3933.
- Orth, W.S., Gillham, R.W., 1996. Dechlorination of trichloroethene in aqueous solution using  $\text{Fe}^0$ . *Environ. Sci. Technol.* 30 (1), 66–71.
- Phillips, D.H., Gu, B., Watson, D.B., Roh, Y., Liang, L., Lee, S.Y., 2000. Performance evaluation of a zerovalent iron reactive barrier: mineralogical characteristics. *Environ. Sci. Technol.* 34 (19), 4169–4176.
- Reardon, E.J., 1995. Anaerobic corrosion of granular iron: measurement and interpretation of hydrogen evolution rates. *Environ. Sci. Technol.* 29 (12), 2936–2945.
- Ritter, K., Odziemkowski, M.S., Gillham, R.W., 2002. An in situ study of the role of surface films on granular iron in the permeable iron wall technology. *J. Contam. Hydrol.* 55, 87–111.
- Roberts, A.L., Totten, L.A., Arnold, W.A., Burris, D.R., Campell, T.J., 1996. Reductive elimination of chlorinated ethylenes by zero-valent metals. *Environ. Sci. Technol.* 30 (8), 2654–2659.
- Weathers, L.J., Parkin, G.F., Alvarez, P.J., 1997. Utilization of cathodic hydrogen as electron donor for chloroform cometabolism by a mixed, methanogenic culture. *Environ. Sci. Technol.* 31 (3), 880–885.
- Wüst, W.F., Köber, R., Schlicker, O., Dahmke, A., 1999. Combined zero and first-order kinetics model of the degradation of TCE and *cis*-DCE with commercial iron. *Environ. Sci. Technol.* 33 (23), 4304–4309.
- Yager, R.M., Bilotta, S.E., Mann, C.L., Madsen, E.L., 1997. Metabolic adaptation and in situ attenuation of chlorinated ethenes by naturally occurring microorganisms in a fractured dolomite aquifer near Niagara Falls, New York. *Environ. Sci. Technol.* 31, 3138–3147.